Stochastic Geometric Modeling and Interference Analysis for Massive MIMO Systems

Prasanna Madhusudhanan, Xing Li, Youjian (Eugene) Liu, Timothy X Brown
Department of Electrical, Computer and Energy Engineering
University of Colorado, Boulder, CO 80309-0425 USA
{mprasanna, xing.li, eugeneliu, timxb}@colorado.edu

***Abstract*—We study a multiple input multiple output (MIMO) cellular system where each base-station (BS) is equipped with a large antenna array and serves some single antenna mobile stations (MSs). With the same setup as in [1], the influence of orthogonal and non-orthogonal pilot sequences on the system performance is analytically characterized when each BS has infinitely many antennas. Using stochastic geometric modeling of the BS and MS locations, closed-form expressions are derived for the distribution of signal-to-interference-ratio (SIR) for both uplink and downlink. Moreover, they are shown to be equivalent for the orthogonal pilots case. Further, it is shown that the downlink SIR is greatly influenced by the correlations between the pilot sequences in the non-orthogonal pilots case. Finally, the mathematical tools can be used to study system performances with other general channel estimation methods and transmission-reception schemes.**

***Index Terms*—Massive MIMO, Poisson point process, Channel estimation, SIR, Achievable rate, Interference analysis.**

I. Introduction

MASSIVE multiple input multiple output (MIMO) systems are multiuser MIMO cellular systems where each base-station (BS) is equipped with a large number of antennas compared to the number of mobile stations (MSs) it serves. The study of such systems has gained immense attention due to their potential for achieving high data rates and throughput gains while ensuring a low transmission powers in both the forward link and reverse link [1]–[3].

In [1], a low complexity transmission-reception scheme is studied for the uplink and downlink performance of such a system. All BSs reuse the same set of orthogonal pilot sequences that they assign to the MSs for reverse link pilot signaling. Using these pilot sequences, the BSs estimate the reverse link channel to the corresponding MS, and extract the subsequent data symbols via maximum ratio combining. Further, due to channel reciprocity enforced by time division duplexing (TDD) operation, the BS also has an estimate of the forward channel, using which the BS does linear precoding prior to downlink data transmission. In the limit as the the number of BS antennas tend towards infinity, in both the uplink and downlink, it was observed that the effect of uncorrelated noise and fast fading is completely eliminated and the desired signal is only corrupted by the interferences caused by a phenomena termed 'pilot contamination', which is due to the reuse of the same set of pilot sequences by all the BSs. Consequently, the distributions of signal-to-interference ratio (SIR) and rate achievable for a given BS-MS pair in both uplink and downlink is studied for the ideal hexagonal cellular system using Monte-Carlo simulations. Further studies in this topic have analyzed different precoder/detector designs with the goal of minimizing the pilot contamination to as low as possible and to analyze the resulting SIR and rate expressions obtained in the uplink and the downlink [4]–[6].

In this paper, we study the massive MIMO system of [1] under stochastic geometric settings and demonstrate that the uplink and downlink performance can be analytically characterized in terms of the key system parameters. Towards this goal, the BS arrangement is modeled according to a homogeneous Poisson point process on the plane, the MSs served by a given BS are uniformly distributed within a circle of a certain fixed radius centered at the BS location and the number of MSs served by each BS is an i.i.d. Poisson random variable with a given mean. This system is depicted in Fig. 1.

The stochastic geometric modeling and analysis of wireless networks has gained increased popularity since they are amenable to rigorous analytical studies [7]–[13]. For the cellular network, a strong motivation for viewing the BS arrangement as a homogeneous Poisson point process can be drawn from the study of the cellular systems in [14]–[16] which suggests that significant insights can be gained by bounding the downlink cellular performance between the ideal hexagonal grid model and the homogeneous Poisson point process based model. More interestingly, in [15, Fig. 2.], it is shown with the help of Monte-Carlo simulations that in the limit of strong log-normal shadow fading (standard deviation of the fading coefficient $\sigma \to \infty$), the downlink SIR distribution of an ideal hexagonal cellular system approaches that of a cellular system with BSs deployed according to a homogeneous Poisson point process.

Recently, the above convergence has been analytically proved in [17, Theorem 3]. It is shown that the downlink performance of a cellular network with any deterministic arrangement of BSs (not just the ideal hexagonal grid model) converges to that of a Poisson point process based model as $\sigma \to \infty$, and moreover even for realistic values of σ (i.e. 8 dB) that are observed in cluttered environments, the latter model is a good approximation for the deterministic model. In the massive MIMO system, the uplink-downlink performance is completely determined by the shadow fading coefficients and the location of the BSs and the MSs in the cellular system, thus making a strong case for a rigorous study of these performance metrics using stochastic geometric models.

The contributions of this paper are briefly described here. Note that the transmission-reception schemes studied in [1]

are restricted to the case where all the pilot sequences were orthogonal to each other. In practice, orthogonality between pilot sequences is hard to ensure in the uplink (downlink) as the MS (BS) transmissions are never perfectly synchronized. In Section III, we have extended it to the more practical case when the pilot sequences have a small correlation with each other, and derived the expressions for the SIR and the achievable rate in both the uplink and downlink for an arbitrary BS-MS pair. Next, in Section IV, closed-form expressions for the distribution of SIR and rate are derived based on the stochastic geometric model. Further, when all the pilot sequences are orthogonal to each other, it is shown that the distribution of SIR and rate in the uplink and downlink are identical. This analytical result is consistent with [2, Fig. 4-7] where the uplink and downlink SIR and rate have nearly identical behavior (see Section IV-A). For the non-orthogonal pilot sequence case (see Section IV-B), closed form expressions for the distribution of the downlink SIR and rate are derived and simple approximations are derived for the corresponding uplink performance. It is shown that the downlink SIR is strictly upper-bounded by the inverse of total pilots correlation.

Next, we introduce the system model.

II. System Model

The cellular system is composed of BSs distributed according to a homogeneous Poisson point process on the plane with BS density λ_b. The BSs employ Δ-frequency reuse (Δ =1, 3, 4, 7 etc.) where each BS is randomly assigned one of the $\{1,\ 2, \cdots,\ \Delta\}$ frequency bands with equal probability and the BSs in different bands do not interfere with each other [18]. Further, the MSs served by a BS are assumed to be uniformly distributed in a circle of radius R centered at the BS and independent of the other MS or BS arrangements. The number of MSs served by a given BS is a Poisson random variable with mean $\lambda_u \pi R^2$, where λ_u is the average number of MSs per cell area. Each MS has a single antenna and each BS is equipped with M antennas ($M \to \infty$). Fig. 1 illustrates the scenario.

All the BSs in the system share the same set of P pilot sequences and can serve at most P MSs simultaneously. Each pilot sequence is a K length unit-norm vector denoted as $\mathbf{a}_i \in \mathbb{C}^{K\times 1}$, $i = 1,\ 2, \cdots, P$, and the correlation between two pilot sequences $\mathbf{a_i},\ \mathbf{a_j}$ is $\mathbf{a_i^\dagger a_j} = \alpha_{ij}$, such that $0 \le |\alpha_{ij}| \le 1$ and $\alpha_{ii} = 1, \forall\ i = 1, \cdots,\ P$. The pilots are said to be orthogonal if the correlation is zero for $i \neq j$ and non-orthogonal otherwise. The BSs and the MSs communicate with each other via time division duplexing (TDD) such that the in-band uplink and downlink transmissions are sufficiently separated in time and do not cause interference to one another. Further, the TDD operation induces channel reciprocity causing the forward and reverse-link channels for a given BS-MS pair to be identical.

III. Transmission-Reception Schemes

This section generalizes the results in [1] to the case when the pilot sequences are non-orthogonal and when the number of MSs in each cell is an independent and identically distributed (i.i.d.) random variable as mentioned in Section II.

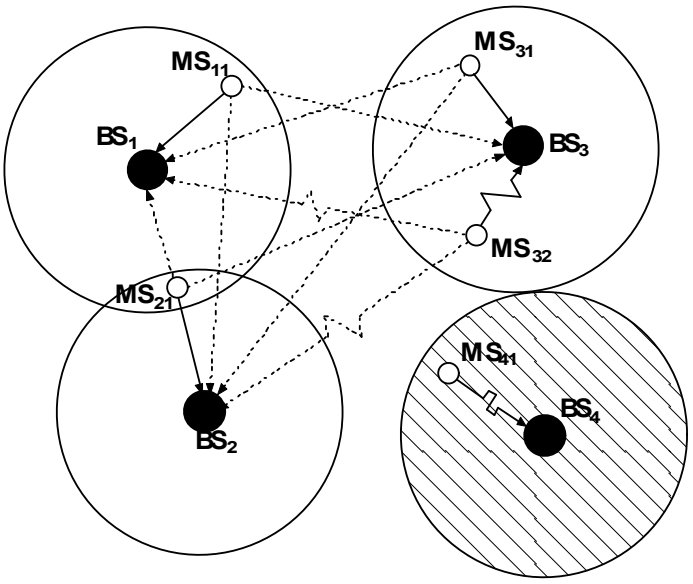

Fig. 1. User distribution and pilots assignments. BSs in the circles with different background patterns operate in different frequency bands. The different pilot sequences assigned to MSs are indicated by different line patterns. Solid line represents desired signal while dotted line represents interference to others.

1) Pilot signaling and channel estimation: The communication begins with the training phase when all the MSs in the cell transmit their respective pilot sequences to the serving BS. The BSs utilize the reverse-link pilot transmissions to estimate the reverse-link channel to each of its MSs. We denote the kth BS by BS_k and its nth MS by MS_{kn}. The received signal at BS_k corresponding to one pilot sequence transmission period (consisting of K symbols) may be represented by $\mathbf{Y}_k \in \mathbb{C}^{M\times K}$:

$$\mathbf{Y}_k = \sqrt{\rho_{\mathrm{P}}} \sum_{l=1}^{\infty} \sum_{n=1}^{P} b_{kl} \mathbf{h}_{kln} \mathbf{a}_n^\dagger \mathcal{I}(n,l) + \mathbf{W}_k \qquad (1)$$

where M is the number of BS antennas, K is the length of a pilot sequence, $b_{kl} = 1$ if BS_l operates in the same frequency band as BS_k and $b_{kl} = 0$ otherwise, $\mathbf{h}_{kln} \in \mathbb{C}^{M\times 1}$ is the channel corresponding to the wireless link from MS_{ln} to BS_k, ρ_{P} is the pilot signal-to-noise ratio (SNR), $\mathbf{W}_k$ is the i.i.d. zero-mean noise at BS_k, and $\mathcal{I}(n,l)$ is the indicator function

$$\mathcal{I}(n,l) = \begin{cases} 1, & n^{\mathrm{th}} \text{ pilot is used in } l^{\mathrm{th}} \text{ cell} \\ 0, & \text{otherwise} \end{cases}.$$

Further, $\mathbf{h}_{kln} = \beta_{kln}^{\frac{1}{2}} R_{kln}^{-\frac{\varepsilon}{2}} \mathbf{g}_{kln}$, $\mathbf{g}_{kln} \in \mathbb{C}^{M\times 1}$ represents the fast fading coefficients between the MS_{ln} and the antennas of BS_k with i.i.d. zero mean and unit variance entries, β_{kln} is the shadow fading coefficient, generally modeled as a log-normal random variable with 0 mean and variance σ^2 dB, R_{kln} is the distance between MS_{ln} and BS_k and ϵ ($\epsilon > 2$) is the path-loss exponent of the power-law path-loss model.

From the received signal in (1), BS_k estimates the channel

to the MS transmitting the m^{th} pilot sequence as

$$\hat{\mathbf{h}}_{kkm} = \frac{\mathbf{Y}_k \mathbf{a}_m}{\sqrt{\rho_{\text{P}}}} = h_{kkm} + \sum_{n=1,\ n\neq m}^{P} \alpha_{nm} \mathbf{h}_{kkn} \mathcal{I}(n,k) + \sum_{l=1,\ l\neq k}^{\infty} \sum_{n=1}^{P} \alpha_{nm} b_{kl} \mathbf{h}_{kln} \mathcal{I}(n,l) + \frac{\mathbf{W}_k \mathbf{a}_m}{\sqrt{\rho_{\text{P}}}}, \quad (2)$$

where $m = 1,\ 2, \cdots,\ P$, the first term is the desired channel, the second term is the contamination due to non-orthogonal pilots used by other MSs served by BS$_k$, the third term is the contamination due to the pilot transmissions of the MSs belonging to the other cells and the last term corresponds to the background noise. Next, we focus on the uplink data transmission and decoding scheme used by each BS to recover the data transmitted by each of its MSs.

2) Uplink Data Transmission and Maximum Ratio Combining: Following the pilot signaling stage is the reverse link data transmission stage, when all the MSs transmit data symbols to their corresponding BS, and the composite signal as received by BS$_k$ is given by

$$\mathbf{y}_k = \sqrt{\rho_{\text{U}}} \sum_{l=1}^{\infty} \sum_{n=1}^{P} b_{kl} \mathbf{h}_{kln} d_{ln} \mathcal{I}(n,l) + \mathbf{w}_k, \quad (3)$$

where ρ_{U} is the uplink SNR, d_{ln} is the data symbol transmitted by MS$_{ln}$, and $\mathbf{w}_k$ is the i.i.d. zero mean and unit variance background noise at BS$_k$'s antennas and all other symbols are the same as in (1). From the above received signal, BS$_k$ recovers the symbols corresponding to each of its MSs using maximum-ratio combining, by left-multiplying the received signal by the conjugate-transpose of the channel estimate of the corresponding MS. Further, in the limit as $M \to \infty$, the recovered data symbol $\hat{d}_{km}$ corresponding to MS$_{km}$ takes a relatively simple form as shown below.

$$\begin{aligned}
\hat{d}_{km} &= \lim_{M\to\infty} \frac{\hat{\mathbf{h}}_{kkm}^{\dagger} \mathbf{y}_k}{M\sqrt{\rho_{\text{U}}}} \\
&\overset{(a)}{=} \lim_{M\to\infty} \frac{1}{M} \left(\sum_{l=1}^{\infty} \sum_{n=1}^{P} \alpha_{nm}^{*} b_{kl} \mathbf{h}_{kln}^{\dagger} \mathcal{I}(n,l) + \frac{\mathbf{a}_m^{\dagger} \mathbf{W}_k^{\dagger}}{\sqrt{\rho_{\text{P}}}} \right) \\
&\quad \cdot \left(\sum_{s=1}^{\infty} \sum_{t=1}^{P} \mathbf{h}_{kst} b_{ks} d_{st} \mathcal{I}(t,s) + \frac{\mathbf{w}_k}{\sqrt{\rho_{\text{U}}}} \right) \\
&\overset{(b)}{=} \frac{\beta_{kkm} d_{km}}{R_{kkm}^{\epsilon}} + \sum_{n=1,\ n\neq m}^{P} \frac{\alpha_{nm}^{*} \beta_{kkn} d_{kn}}{R_{kkn}^{\epsilon}} \mathcal{I}(n,k) \\
&\quad + \sum_{l=1,\ l\neq k}^{\infty} \sum_{n=1}^{P} \frac{\alpha_{nm}^{*} b_{kl} \beta_{kln} d_{ln}}{R_{kln}^{\epsilon}} \mathcal{I}(n,l), \quad (4)
\end{aligned}$$

where $m = 1,\ 2, \cdots,\ P$, (a) is obtained by substituting for $\hat{\mathbf{h}}_{kkm}$ and $\mathbf{y}_k$ from (2) and (3), respectively, and (b) is obtained by noting that $\lim_{M\to\infty} \frac{\mathbf{h}_{kln}^{\dagger} \mathbf{h}_{kst}}{M} = \sqrt{\frac{\beta_{kln}\beta_{kst}}{R_{kln}^{\frac{\epsilon}{2}} R_{kst}^{\frac{\epsilon}{2}}}} \lim_{M\to\infty} \frac{\mathbf{g}_{kln}^{\dagger} \mathbf{g}_{kst}}{M}$ $= b_{kl}\beta_{kln} R_{kln}^{-\epsilon} \delta(l=s, n=t)$, $\lim_{M\to\infty} \frac{\mathbf{h}_{kln}^{\dagger} \mathbf{w}_k}{M} = 0$, $\lim_{M\to\infty} \frac{\mathbf{W}_k^{\dagger} \mathbf{h}_{kst}}{M} = 0$, and $\lim_{M\to\infty} \frac{\mathbf{W}_k^{\dagger} \mathbf{w}_k}{M} = 0$ by applying the law of large numbers, since $\mathbf{g}_{kln}$, $\mathbf{w}_k$, $\mathbf{W}_k$ all contain i.i.d. zero mean unit variance entries. Further, the first term in (b) is the desired data symbol, the second is the intra-cell interference term and the third is the inter-cell interference term. Next, we study the downlink transmission scheme in detail.

3) Precoding and Downlink Data Transmission: In the downlink, the BS precodes the data symbol intended for each MS with the channel estimate of the corresponding wireless link, and transmits the sum of the precoded signals of all its MSs through the M antennas. The received signal at MS$_{km}$ is

$$y_{km} = \sqrt{\rho_{\text{D}}} \sum_{l=1}^{\infty} b_{kl} \mathbf{h}_{lkm}^{\dagger} x_l + w_{km},$$

where ρ_{D} is the downlink SNR, $x_l = \sum_{n=1}^{P} \hat{\mathbf{h}}_{lln} d_{ln} \mathcal{I}(n,l)$ is the signal transmitted by BS$_l$, d_{ln} is the data symbol intended to MS$_{ln}$ and is precoded by the corresponding channel estimate $\hat{\mathbf{h}}_{lln}$. Due to channel reciprocity induced by the TDD operation, the channel between BS$_l$ and MS$_{km}$ is $\mathbf{h}_{lkm}^{\dagger}$, and lastly, w_{km} is a zero mean, unit variance random variable representing the background noise. Each MS performs a relatively simple processing to recover the data symbol transmitted by the serving BS. The recovered data symbol in the downlink is

$$\begin{aligned}
\hat{d}_{km} &= \lim_{M\to\infty} \frac{y_{km}}{M\sqrt{\rho_{\text{D}}}} \\
&= \lim_{M\to\infty} \frac{1}{M} \sum_{l=1}^{\infty} \mathbf{h}_{lkm}^{\dagger} \sum_{n=1}^{P} \hat{\mathbf{h}}_{lln} d_{ln} \mathcal{I}(n,l) + \frac{w_{km}}{M\sqrt{\rho_{\text{D}}}} \\
&= \sum_{l=1}^{\infty} \left(\sum_{n=1}^{P} \alpha_{nm}^{*} d_{ln} \mathcal{I}(n,l) \right) b_{kl} \beta_{lkm} R_{lkm}^{-\epsilon}, \quad (5)
\end{aligned}$$

where $m = 1,\ 2, \cdots,\ M$, $\lim_{M\to\infty} \frac{\mathbf{h}_{lkm}^{\dagger} \hat{\mathbf{h}}_{lln}}{M} = \alpha_{mn}\beta_{lkm} R_{lkm}^{-\epsilon}$, $\alpha_{mn} = \alpha_{nm}^{*}$, and $\lim_{M\to\infty} \frac{w_{km}}{M\sqrt{\rho_{\text{D}}}} = 0$. Notice that the resultant system is again interference-limited and the following lemma provides the expressions for the uplink and downlink SIR for a given BS-MS pair.

Lemma 1. *The uplink and downlink SIRs are*

$$\textit{SIR}_{km}^{(UL)} = \frac{\beta_{kkm}^2 R_{kkm}^{-2\epsilon}}{I_{km}^{(UL)}} \text{ and } \textit{SIR}_{km}^{(DL)} = \frac{\beta_{kkm}^2 R_{kkm}^{-2\epsilon}}{I_{km}^{(DL)}}, \quad (6)$$

where $I_{km}^{(UL)} = \sum_{l=1}^{\infty} \sum_{\substack{n=1 \\ (l,n)\neq(k,m)}}^{P} b_{kl} |\alpha_{nm}|^2 \beta_{kln}^2 R_{kln}^{-2\epsilon} \mathcal{I}(n,l)$ *and* $I_{km}^{(DL)} = \sum_{l=1}^{\infty} \Big(\sum_{\substack{n=1 \\ (l,n)\neq(k,m)}}^{P} |\alpha_{nm}|^2 \mathcal{I}(n,l) \Big) b_{kl} \beta_{lkm}^2 R_{lkm}^{-2\epsilon}$ *are the corresponding interference powers.*

Notice that, when each BS serves a fixed number of user equal to P using a set of P orthogonal pilot sequences, the resultant expressions for $\text{SIR}_{km}^{(UL)}$ and $\text{SIR}_{km}^{(DL)}$ are identical to those obtained in [1].

In the following section, we systematically evaluate the system performance in the uplink and downlink.

IV. Interference characteristics and SIR

In this section, we derive closed-form expressions for the Laplace transform of interference and the SIR distribution for

both uplink and downlink. We first consider the case when all the P pilot sequences are orthogonal to each other. Since each pilot sequence is of length K, at most K orthogonal pilot sequences can be designed, and hence $P \leq K$.

A. Case of orthogonal pilot sequences

In this case, the pilot sequences $a_1, \cdots, a_P$ are such that the correlation $\alpha_{ij} = 1$, if $i = j$ and 0 otherwise. From Lemma 1, it can be seen that the intra-cell interference is completely eliminated and the inter-cell interference is only due to the transmissions corresponding to the same pilot sequence as the desired signal.

Theorem 2. *With orthogonal pilot sequences, the Laplace transform of the interference in the uplink and downlink are*

$$\mathcal{L}_{I_{km}^{(UL)}} = \mathcal{L}_{I_{km}^{(DL)}}(s) = \exp\left(-\frac{\lambda_b \pi \eta \mathbb{E}\left[\beta^{\frac{2}{\epsilon}}\right] s^{\frac{1}{\epsilon}}}{\Gamma\left(1+\frac{1}{\varepsilon}\right) \Delta \mathrm{sinc}\left(\frac{\pi}{\epsilon}\right)}\right), \tag{7}$$

where $\Gamma(\cdot)$ is the Gamma function, $I_{km}^{(UL)}$ and $I_{km}^{(DL)}$ are obtained from Lemma 1, $\eta = \sum_{n=1}^{P-1} \frac{n}{P} \frac{\left(\lambda_u \pi R^2\right)^n}{n!} e^{-\lambda_u \pi R^2} + \sum_{n=P}^{\infty} \frac{\left(\lambda_u \pi R^2\right)^n}{n!} e^{-\lambda_u \pi R^2}$ is the probability that two BSs in the system use the same pilot sequence, β is the random variable with the same distribution as the set of i.i.d. random variables $\{\beta_{klm}\}_{l=1}^{\infty}$, $\mathbb{E}\left[\beta^{\frac{2}{\epsilon}}\right] < \infty$, Δ is the frequency reuse factor and $\mathrm{sinc}(x) = \frac{\sin(x)}{x}$. Also,

$$SIR_{km}^{(UL)} =_{st} SIR_{km}^{(DL)}, \tag{8}$$

where $=_{\mathrm{st}}$ is the equivalence in distribution. Further, in the special case when $\{\beta_{klm}\}_{l=1}^{\infty}$ is a set of i.i.d. unit mean exponential random variables, the complementary cumulative density function (c.c.d.f.) of SIR is

$$\mathbb{P}\left(\left\{\mathrm{SIR}_{km}^{(UL)} > \gamma\right\}\right) = \mathbb{P}\left(\left\{\mathrm{SIR}_{km}^{(DL)} > \gamma\right\}\right) = \frac{1 - \mathrm{e}^{-T}}{T}, \tag{9}$$

where $\gamma \geq 0$ and $T = \frac{\eta \lambda_b \pi R^2 \gamma^{\frac{1}{\epsilon}}}{\Delta \mathrm{sinc}\left(\frac{\pi}{\epsilon}\right)}$.

Proof: See Appendix A. ∎

Further, when the number of users in each cell is equal to K at all times, all $P = K$ orthogonal pilot sequences are used by each BS, η (defined in Theorem 2) is 1 and hence the c.c.d.f. of SIR is obtained using (9) with $\eta = 1$. Note that the above is exactly the scenario considered in [1] where the uplink and downlink SIRs could only be analyzed via Monte-Carlo simulations. Here, with the help of stochastic geometry, we are able to obtain closed form expressions for the relevant performance metrics in terms of the critical system parameters. In Section V, we further demonstrate its significance with numerical examples.

B. Case of non-orthogonal pilot sequences

Now, we consider the case when the pilot sequences are not orthogonal to each other. Such a scenario arises under two conditions. Firstly, when the pilot signaling by various transmitters are not perfectly synchronized. Secondly, in an overloaded system where the BS serves a large number of users. Particularly when $P > K$, all P pilot sequences of length K cannot be orthogonal to each other. In this section, we consider an extreme case when all the P pilot sequences are used by each BS. The uplink and downlink interferences ar

$$I_{km}^{(UL)} = \sum_{\substack{l=1 \\ (l,n)\neq(k,m)}}^{\infty} \sum_{n=1}^{P} b_{kl} \left|\alpha_{nm}\right|^2 \beta_{kln}^2 R_{kln}^{-2\epsilon}, \tag{10}$$

$$I_{km}^{(DL)} = \frac{\bar{\alpha}_m \beta_{kkm}^2}{R_{kkm}^{2\epsilon}} + (\bar{\alpha}_m + 1) \sum_{l=1,\ l\neq k}^{\infty} \frac{b_{kl} \beta_{lkm}^2}{R_{lkm}^{2\epsilon}}, \tag{11}$$

where $\bar{\alpha}_m \triangleq \sum_{\substack{n=1 \\ n\neq m}}^{P} \left|\alpha_{nm}\right|^2$. By substituting in (6), we obtain the corresponding SIR expressions. The following theorem derives the Laplace transform of interference and the distribution of SIR in the downlink.

Theorem 3. *When all BSs in the system serve P MSs using the P non-orthogonal pilot sequences, the Laplace transform of the $I_{km}^{(DL)}$ is*

$$\mathcal{L}_{I_{km}^{(DL)}}(s) = \mathbb{E}_{\beta}\left[\frac{\left(s\bar{\alpha}_m \beta^2\right)^{\frac{1}{\epsilon}} \Gamma\left(-\frac{1}{\epsilon}, \frac{s\bar{\alpha}_m \beta^2}{R^{2\epsilon}}\right)}{\epsilon R^2}\right] \times \exp\left(-\frac{\lambda_b \pi \mathbb{E}\left[\beta^{\frac{2}{\epsilon}}\right] s^{\frac{1}{\epsilon}} \left(\bar{\alpha}_m + 1\right)^{\frac{1}{\epsilon}}}{\Gamma\left(1+\frac{1}{\varepsilon}\right) \Delta \mathrm{sinc}\left(\frac{\pi}{\epsilon}\right)}\right), \tag{12}$$

where $\Gamma(\cdot,\cdot)$ is the incomplete Gamma function, $\Gamma(\cdot)$ is the Gamma function, β is a random variable with the same distribution as the i.i.d. random variables β_{klm}'s in (11), Δ and $\mathrm{sinc}(\cdot)$ are as in Theorem 2.

When $\{\beta_{klm}\}_{l=1}^{\infty}$ is a set of i.i.d. unit mean exponential random variables, the c.c.d.f. of downlink SIR is

$$\mathbb{P}\left(\left\{\mathrm{SIR}_{km}^{(DL)} > \gamma\right\}\right) = \frac{\Delta \mathrm{sinc}\left(\frac{\pi}{\epsilon}\right)}{\lambda_b \pi R^2 \bar{\gamma}^{\frac{1}{\epsilon}}} \left[1 - \mathrm{e}^{-\frac{\lambda_b \pi R^2 \bar{\gamma}^{\frac{1}{\epsilon}}}{\Delta \mathrm{sinc}\left(\frac{\pi}{\epsilon}\right)}}\right], \tag{13}$$

$\forall\ 0 \leq \gamma \leq \bar{\alpha}_m^{-1}$ *and* $\bar{\gamma} = \frac{\gamma(1+\bar{\alpha}_m)}{1-\bar{\alpha}_m \gamma}$.

Proof: See Appendix B. ∎

An important implication of Theorem 3 is that the downlink SIR in the non-orthogonal case cannot exceed $\frac{1}{\bar{\alpha}_m}$ as can be seen from (19), and hence shows how the design of the set of pilot sequences determines the system performance.

Next, we characterize the uplink performance with non-orthogonal pilot sequences. Accurate closed-form characterizations of the performance metrics in the uplink is not possible, and hence, we consider the following approximations to (10) that make the analysis tractable.

1) Replace the instantaneous correlation between the pilot sequences with the average of the correlations with all pilot sequences, i.e. replace $\left|\alpha_{nm}\right|^2$ of the intra-cell interference terms with $\frac{\bar{\alpha}_m}{P-1}$ and $\left|\alpha_{nm}\right|^2$ of the inter-cell interference terms with $\frac{\bar{\alpha}_m+1}{P}$.

2) Upper bound the distance between MS_{ln} and BS_k, R_{kln} with $R_{kl}+R$, for $(l,n)\neq(k,m)$, where R_{kl} is the radial distance between BS_k and BS_l. By doing so, it can be shown that the point process of the resultant inter-cell interferer is a homogeneous Poisson point process in the entire plane except the circle of radius R about the origin. Further, the resultant interference after this operation is a lower bound for the actual uplink interference.
3) In order to achieve a mathematically tractable approximation, we extend the interferer point process obtained by the previous operation to the entire plane.

With the above three modifications, a reasonable estimate for the uplink interference is obtained as

$$\hat{I}_{km}^{(UL)} = \frac{\bar{\alpha}_m R^{-2\epsilon}}{P-1} \sum_{n=1,\ n\neq m}^{P} \beta_{kkn}^2 + \frac{(\bar{\alpha}_m+1)}{P} \sum_{l=1,\ l\neq k}^{\infty} b_{kl} \left(\sum_{n=1}^{P} \beta_{kln}^2\right) R_{kl}^{-2\epsilon}, \quad (14)$$

where R_{kkn}'s are i.i.d. random variables with a probability density function (p.d.f.) $f_{R_{kkn}}(r) = \frac{2r}{R^2},\ 0\leq r\leq R$, R_{kl}'s are from the homogeneous Poisson point process on the plane with density λ_b and β_{kln}'s are i.i.d. random shadow fading factors, and the corresponding uplink SIR is

$$\hat{\mathrm{SIR}}_{km}^{(UL)} = \frac{\beta_{kkm}^2 R_{kkm}^{-\varepsilon}}{\hat{I}_{km}^{(UL)}}. \quad (15)$$

Using (14) and (15), next we derive analytical expressions for the uplink performance metrics.

Theorem 4. *The Laplace transform of $\hat{I}_{km}^{(UL)}$ is*

$$\mathcal{L}_{\hat{I}_{km}^{(UL)}}(s) = \left(\mathbb{E}_\beta\left[\mathrm{e}^{-\frac{s\bar{\alpha}_m R^{-2\epsilon}\beta^2}{P-1}}\right]\right)^{P-1} \times \exp\left(-\frac{\lambda_b \mathbb{E}\left[\left(\sum_{n=1}^{P}\beta_n^2\right)^{\frac{1}{\epsilon}}\right] s^{\frac{1}{\epsilon}} (\bar{\alpha}_m+1)^{\frac{1}{\epsilon}}}{P^{\frac{1}{\varepsilon}}\Gamma\left(1+\frac{1}{\varepsilon}\right)\Delta \mathrm{sinc}\left(\frac{\pi}{\epsilon}\right)}\right), \quad (16)$$

where β, $\{\beta_n\}_{n=1}^P$ are i.i.d. random variables with the same distribution as β_{kln}'s in (14), Δ and $\mathrm{sinc}(\cdot)$ are as in Theorem 2. When $\{\beta_{klm}\}_{l=1}^{\infty}$ is a set of i.i.d. unit mean exponential random variables, the c.c.d.f. of uplink SIR using the approximation (14) is

$$\mathbb{P}\left(\left\{\hat{\mathrm{SIR}}_{km}^{(UL)} > \gamma\right\}\right) = \mathbb{E}_{R_{kkm}}\left[\mathcal{L}_{\hat{I}_{km}^{(UL)}}\left(\gamma R_{kkm}^{2\epsilon}\right)\right] \quad (17)$$

Proof: Equation (16) can be obtained by following the same steps as for the derivation of (12), and (17) is obtained by substituting for $\hat{\mathrm{SIR}}_{km}^{(UL)}$ from (15) and then evaluating the probability w.r.t. β_{kkm}^2, given all other random variables. ■

Next, the per-user achievable rate (in bits/secs/user) in the uplink and downlink are

$$R_{km}^{(UL)} = \frac{B\rho}{\Delta}\log_2\left(1+\mathrm{SIR}_{km}^{(UL)}\right) \text{ and}$$
$$R_{km}^{(DL)} = \frac{B\rho}{\Delta}\log_2\left(1+\mathrm{SIR}_{km}^{(DL)}\right),$$

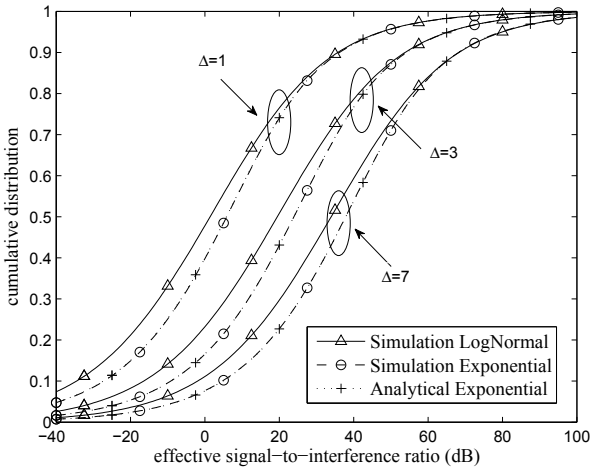

Fig. 2. Cumulative distribution for the effective signal-to-interference ratio in fully loaded MS case with orthogonal pilots.

respectively, where B is the entire allocated bandwidth, ρ is the scaling factor for the rate-loss from training, guard interval, etc. and Δ is the frequency reuse factor. The above are the uplink and downlink Shannon rates obtained by treating interference as noise.

The c.c.d.f. of $R_{km}^{(UL)}$ and $R_{km}^{(DL)}$ for both the orthogonal and non-orthogonal pilots cases can be obtained from Theorems 2-4 by replacing γ in equations (9), (13) and (17) with $\exp\left(\frac{\gamma\Delta}{B\rho}\right)-1$.

Next, we provide some numerical examples that further demonstrate the utility of the analytical study carried out in this section.

V. Numerical Results

In order to facilitate a fair comparison between the analytical results obtained in the previous section with the empirical results in [1, Section VI], we restrict our attention to the orthogonal pilots case (Section IV-A) and assume the same system parameters as in [1, Section VI]. From Theorem 2, the uplink and downlink performances are identical and the hence the conclusions drawn in this section hold true for both.

Simulation setting: The cellular area of interest is a circle with a radius 50 kilometers with the radius of each cell $R=1600$ meters and BSs distributed according to a homogeneous Poisson point process with density $\lambda_b = \frac{1}{\pi R^2}$. The total system bandwidth $B=20$ MHz, and the rate scaling factor $\rho = (3/7)\times(66.7/71.4)\approx 0.4$. Three different values for the frequency reuse factors are considered, $\Delta = 1,\ 3$ and 7, and all the BSs reuse $K=42$ orthogonal pilot sequences among themselves. For the shadow-fading, two cases are considered: (a) β_{klm}'s follow i.i.d. log-normal distribution with 8.0 dB standard deviation as in [1], and (b) β_{klm}^2's follow i.i.d. unit mean exponential distribution, and finally the path-loss exponent $\epsilon = 3.8$.

Fully loaded case: Fig. 2 and Fig. 3 show the cumulative distributions for the SIR (8) and the average achievable rate per user, respectively, when every cell is fully loaded and serving

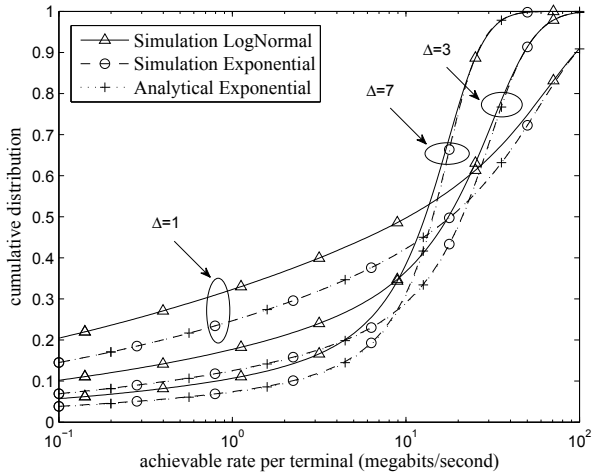

Fig. 3. Cumulative distribution for the net achievable rate per terminal in fully loaded MS case with orthogonal pilots.

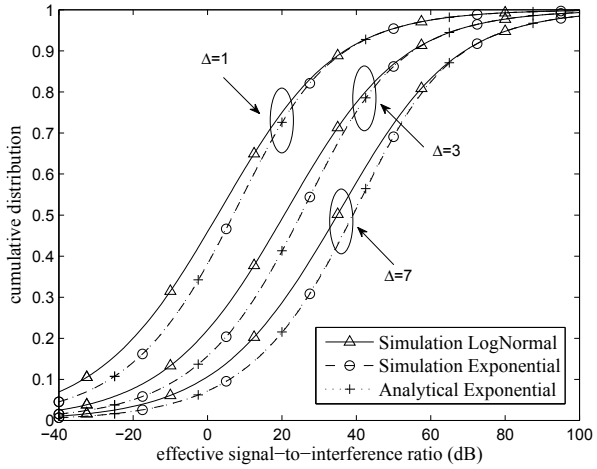

Fig. 4. Cumulative distribution for the effective signal-to-interference ratio in random MS case with orthogonal pilots.

its maximum capacity of P users. Note that the analytical results obtained from (9) with $\eta = 1$ fits the simulation result perfectly. Further, the performance characteristics of the the exponential and the log-normal fading cases are similar. The SIR performance strictly improves as Δ increases because the average interferer distance increases with Δ. The net achievable rate per terminal doesn't necessarily increase as shown in Fig. 3 since larger Δ means smaller effective bandwidth per cell. Hence, Δ should be accordingly chosen based on the minimum or average rate and SIR requirements.

Further, comparing Figs. 3 - 5 with [1, Figs. 2-5], we see that the performances in the hexagonal grid model and the stochastic geometric model are very close to each other. Hence, stochastic geometry based model can provides accurate analytical performance characterizations for these cellular systems.

Random MS case with orthogonal pilots: Now, consider the case when the number of MSs in each cell is a Poisson random variable with mean P. When there are more than P MSs in the cell, only P of them are served. Thus, the desired BS will only receive interference from the cells that are using the same pilot as the desired MS.

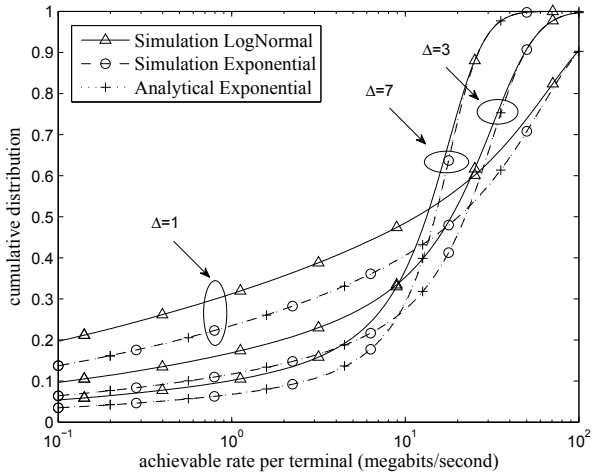

Fig. 5. Cumulative distribution for the net achievable rate per terminal in random MS case with orthogonal pilots.

Fig. 4 and Fig. 5 show the cumulative distributions for the SIR and the average achievable rate per user, respectively. Again, the analytical results using (9) fits the simulation perfectly. Also noticed that although the average number of MSs in the cell are same for both cases, the average served MS number is smaller for the random MS case since we can only serve at most P MSs at the same time. Therefore, the overall performance of this case is better than the fully loaded case considered previously.

VI. Conclusion and Future Works

Massive MIMO system in which base stations are equipped with large numbers of antennas has the potential to deliver enhanced throughput and reliably on both the uplink and downlink in a fast-changing propagation environments [1]. As the number of antennas in the BS tends to infinity, one BS can serve an arbitrary number of MSs at arbitrary high rate as long as accurate channel state information is available. The capacity of the massive MIMO system is highly limited by the accuracy of channel state information and hence the channel estimation method plays a key role. Trade-offs such as total number of pilots vs their correlations between each other need to be thoroughly understood to achieve the best overall performance. Good mathematical tools are necessary to evaluate the system performance with different settings and schemes.

We adopt stochastic geometry to model the BS and MS locations in the cellular system and derive analytical characterizations for the cellular performance in terms of the key system parameters. When using orthogonal pilots, the closed-form expressions for the Laplace transform of interference and the distributions of SIR and achievable rates are obtained and a duality between the distributions of uplink and downlink SIR is revealed. For non-orthogonal pilots case, it is shown that downlink SIR is strictly limited by the inverse of the

total pilot correlation and a reasonable estimates for the uplink performance are derived.

Finally, note that the uplink-downlink performance is mainly determined by the interference caused to the link due to pilot contamination. The mathematical tools developed here can be used to study the system performance under other different channel estimation methods and transmission-reception schemes, such as those studied in [4]–[6].

REFERENCES

[1] T. Marzetta, "Noncooperative cellular wireless with unlimited numbers of base station antennas," *IEEE Transactions on Wireless Communications*, vol. 9, no. 11, pp. 3590 –3600, Nov 2010.

[2] ——, "How much training is required for multiuser MIMO?" in *40th Asilomar Conference on Signals, Systems and Computers*, Nov 2006, pp. 359 –363.

[3] F. Rusek, D. Persson, B. K. Lau, E. Larsson, T. Marzetta, O. Edfors, and F. Tufvesson, "Scaling up MIMO: Opportunities and challenges with very large arrays," *IEEE Signal Processing Magazine*, vol. 30, no. 1, pp. 40 –60, Jan 2013.

[4] J. Hoydis, S. ten Brink, and M. Debbah, "Massive MIMO in the UL/DL of cellular networks: How many antennas do we need?" *IEEE Journal on Selected Areas in Communications*, vol. 31, no. 2, pp. 160–171, Feb 2013.

[5] A. Ashikhmin and T. Marzetta, "Pilot contamination precoding in multi-cell large scale antenna systems," in *IEEE International Symposiumon Information Theory Proceedings (ISIT)*, July 2012, pp. 1137–1141.

[6] J. Jose, A. Ashikhmin, T. Marzetta, and S. Vishwanath, "Pilot contamination and precoding in multi-cell tdd systems," *IEEE Transactions on Wireless Communications*, vol. 10, no. 8, pp. 2640–2651, Aug 2011.

[7] P. Madhusudhanan, J. G. Restrepo, Y. Liu, T. X. Brown, and K. R. Baker, "Downlink performance analysis for a generalized shotgun cellular system," *CoRR*, 2010. [Online]. Available: http://arxiv.org/abs/1002.3943

[8] P. Madhusudhanan, J. G. Restrepo, Y. Liu, T. X. Brown, and K. Baker, "Stochastic ordering based carrier-to-interference ratio analysis for the shotgun cellular systems," *IEEE Wireless Communications Letters*, vol. PP, no. 99, pp. 1 –4, 2012.

[9] P. Madhusudhanan, J. G. Restrepo, Y. Liu, and T. X. Brown, "Downlink coverage analysis in a heterogeneous cellular network," *CoRR*, 2012. [Online]. Available: http://arxiv.org/abs/1206.4723

[10] H. S. Dhillon, R. K. Ganti, F. Baccelli, and J. G. Andrews, "Modeling and analysis of K-tier downlink heterogeneous cellular networks," *IEEE Journal on Selected Areas in Communications*, vol. 30, no. 3, pp. 550 –560, Apr 2012.

[11] V. M. Nguyen and F. Baccelli, "A stochastic geometry model for the best signal quality in a wireless network," in *8th International Symposium on Modeling and Optimization in Mobile, Ad Hoc and Wireless Networks (WiOpt)*, Jun 2010, pp. 465 –471.

[12] W. Yu-Chun, W. Haiguang, and P. Zhang, "Protection of Wireless Microphones in IEEE 802.22 Cognitive Radio Network," *IEEE International Conference on Communications Workshops*, pp. 1 –5, Jun 2009.

[13] C.-H. Lee and M. Haenggi, "Interference and Outage in Poisson Cognitive Networks," *IEEE Transactions on Wireless Communications*, 2012. [Online]. Available: http://www.nd.edu/ mhaenggi/pubs/twc12.pdf

[14] T. X. Brown, "Analysis and coloring of a shotgun cellular system," *IEEE Radio and Wireless Conference (RAWCON)*, pp. 51–54, Aug 1998.

[15] ——, "Cellular performance bounds via shotgun cellular systems," *IEEE Journal on Selected Areas in Communications*, vol. 18, no. 11, pp. 2443–2455, Nov 2000.

[16] J. Andrews, F. Baccelli, and R. Ganti, "A tractable approach to coverage and rate in cellular networks," *IEEE Transactions on Communications*, vol. 59, no. 11, pp. 3122 –3134, Nov 2011.

[17] B. Blaszczyszyn, M. K. Karray, and H.-P. Keeler, "Using Poisson processes to model lattice cellular networks," *CoRR*, 2012. [Online]. Available: http://arxiv.org/abs/1207.7208

[18] T. S. Rappaport, *Wireless Communications: Principles and Practice*. Upper Saddle River, NJ, USA: Prentice-Hall, Inc., 1996.

[19] M. Haenggi and R. K. Ganti, "Interference in Large Wireless Networks," *Foundations and Trends in Networking*, vol. 3, no. 2, pp. 127–248, 2008, available at http://www.nd.edu/ mhaenggi/pubs/now.pdf. [Online]. Available: http://www.nd.edu/ mhaenggi/pubs/now.pdf

[20] J. F. C. Kingman, *Poisson Processes (Oxford Studies in Probability)*. Oxford University Press, USA, January 1993.

APPENDIX

A. Proof for Theorem 2

In the orthogonal pilots case, $\alpha_{ij} = \begin{cases} 1, & i=j \\ 0, & i \neq j \end{cases}$. By substituting for α_{ij} in Lemma 1, we get $I_{km}^{(UL)} = \sum_{l=1,\ l\neq k}^{\infty} b_{kl}\beta_{klm}^2 R_{klm}^{-2\epsilon}\mathcal{I}(m,l)$, $I_{km}^{(DL)} = \sum_{l=1,\ l\neq k}^{\infty} b_{kl}\beta_{lkm}^2 R_{lkm}^{-2\epsilon}\mathcal{I}(m,l)$ and by substituting these into (6), the uplink and downlink SIR expressions are obtained. Note that $I_{km}^{(DL)}$ is the interference at MS_{km} due to BS_l transmissions $(l \neq k)$ to MS_{lm}. Using Slivnyak's theorem [19], the Palm distribution of all the BSs conditioned on the location of BS_k serving MS_{km} is also a Poisson point process and using Campbell's theorem [20, Page 57], the Laplace transform of $I_{km}^{(DL)}$ is equal to (7).

On the other hand, $I_{km}^{(UL)}$ is the interference at BS_k (assumed to be at the origin) from MSs using the m^{th} pilot sequence served by other BSs that operate in the same frequency band as BS_k. Using the same argument as before, all the other BSs in the cellular system given BS_k is at the origin is also a homogeneous Poisson point process with BS density λ_b. Hence, the Laplace transform of $I_{km}^{(UL)}$can be expressed as

$$
\begin{aligned}
&\mathcal{L}_{I_{km}^{(UL)}}(s) \\
&\overset{(a)}{=} \mathbb{E}\left[\prod_{l=1,\ l\neq k}^{\infty} \mathrm{e}^{-sb_{kl}\beta_{klm}^2\|X_l+Y_{lm}\|^{-2\varepsilon}\mathcal{I}(m,l)}\right] \\
&\overset{(b)}{=} \exp\left(-\frac{\lambda_b\eta}{\Delta}\int_{x\in\mathbb{R}^2}\mathbb{E}_{\beta,Y}\left[1-\mathrm{e}^{-s\beta^2\|x+Y\|^{-2\varepsilon}}\right]dx\right) \\
&\overset{(c)}{=} \exp\left(-\frac{\lambda_b\eta}{\Delta}\mathbb{E}_{\beta,Y_1,Y_2}\left[\iint_{x_1=-\infty,\ x_2=-\infty}^{x_1=\infty,\ x_2=\infty}\right.\right. \\
&\left.\left.\left(1-\mathrm{e}^{-s\beta^2\left[(x_1+Y_1)^2+(x_2+Y_2)^2\right]^{-\varepsilon}}\right)dx_1dx_2\right]\right) \\
&\overset{(d)}{=} \mathrm{e}^{-\frac{\lambda_b\eta}{\Delta}\mathbb{E}_\beta\left[\int_{r=0}^{\infty}\left(1-\mathrm{e}^{-sb_k\beta^2r^{-2\epsilon}\mathcal{I}(m,l)}\right)2\pi rdr\right]} \\
&\overset{(e)}{=} \exp\left(-\frac{\pi\eta\lambda_b}{\Delta}s^{\frac{1}{\epsilon}}\cdot\mathbb{E}\left[\beta^{\frac{2}{\epsilon}}\right]\cdot\int_0^{\infty}\left(e^{-t^{-\epsilon}}-1\right)\mathrm{d}t\right) \qquad (18)
\end{aligned}
$$

where (a) is obtained by rewriting $I_{km}^{(UL)}$ in terms of the locations of BS_l denoted by $X_l \in \mathbb{R}^2$, and the location of MS_{lm} around BS_l denoted by $\{Y_{lm}\}_{l=1}^{\infty} \in \mathbb{R}^2$ which is i.i.d. uniformly distributed in the circle of radius R around the origin, (b) is obtained by first evaluating the expectation w.r.t. b_{kl}'s that are i.i.d. Bernoulli$\left(\frac{1}{\Delta}\right)$ random variables and the indicator functions $\mathcal{I}(m,l)$ such that $\mathbb{E}[\mathcal{I}(m,l)] = \eta = \sum_{n=1}^{P-1}\frac{n}{P}\frac{\left(\lambda_u\pi R^2\right)^n}{n!}e^{-\lambda_u\pi R^2} + \sum_{n=P}^{\infty}\frac{\left(\lambda_u\pi R^2\right)^n}{n!}e^{-\lambda_u\pi R^2}$ is the probability that BS_l is currently using the m^{th} pilot sequence $\forall\ l \neq k$ and then applying Campbell's theorem [20, Page 57] to the Poisson point process of the BS arrangement where the expectation operator is w.r.t. the random variable β which has the same distribution as β_{klm}'s, (c) is obtained by exchanging the order of expectation and integration and expressing the integral over $\mathbb{R}^2$ in the Cartesian coordinate system, (d) is obtained by the following variable changes: $x_1 \leftarrow x_1 + Y_1$ and $x_2 \leftarrow x_2 + Y_2$ and rewriting the integrals in the polar coordinate system, (e) is obtained by a variable change $t \leftarrow \beta^{-\frac{2}{\epsilon}}r^2$ and then evaluating the expectation w.r.t.

β, and finally, (7) is obtained by rewriting the integral in (e) in terms of $\mathrm{sinc}\,(\cdot)$.

Now, since $\mathcal{L}_{I_{km}^{(UL)}}(s) = \mathcal{L}_{I_{km}^{(DL)}}(s)$, the $I_{km}^{(UL)}$ and $I_{km}^{(DL)}$ have the same distribution. Further, since the numerator and denominator in the SIR expressions in (6) are independent of each other, it is clear that the distribution of SIR in the uplink and downlink are also identical, and hence we have (8).

Next, if $\left\{\beta_{klm}^2\right\}_{l=1}^{\infty}$ is a set of i.i.d. unit mean exponential random variables, the c.c.d.f. of $\mathrm{SIR}_{km}^{(DL)}$ is

$$\begin{aligned}
&\mathbb{P}\left(\left\{\mathrm{SIR}_{km}^{(DL)} > \gamma\right\}\right)\\
&\overset{(a)}{=} \mathbb{E}\left[\mathrm{e}^{-\gamma R_{kkm}^{2\epsilon}\sum_{l=1,\ l\neq k}^{\infty} b_{kl}\beta_{klm}^2 R_{klm}^{-2\epsilon}\mathcal{I}(m,l)}\right]\\
&\overset{(b)}{=} \mathbb{E}_{R_{kkm}}\left[\mathrm{e}^{-\frac{\lambda_b\eta}{\Delta}\int_0^{\infty}\left(1-\mathbb{E}_{\beta^2}\left[e^{-\gamma R_{kkm}^{2\epsilon}\beta^2 r^{-2\epsilon}}\right]\right)2\pi r\mathrm{d}r}\right]\\
&\overset{(c)}{=} \mathbb{E}_{R_{kkm}}\left[\exp\left(-\frac{\eta\gamma^{\frac{1}{\epsilon}}\lambda_b\pi R_{kkm}^2}{\Delta\mathrm{sinc}\left(\frac{\pi}{\epsilon}\right)}\right)\right],
\end{aligned}$$

where $\gamma \geq 0$, (a) is obtained by evaluating the probability w.r.t. the unit mean exponential random variable β_{kkm}^2 conditioned on all other random variables, (b) is similar to (18-(b)), (c) is obtained by evaluating the expectation w.r.t. β^2 which is a unit mean exponential random variable and then evaluating the integral in (b) and finally, (9) is obtained by evaluating the expectation w.r.t. $R_{kkm}$with the probability density function $f_{R_{kkm}}(r) = \begin{cases}\frac{2r}{R^2} & 0 \leq r \leq R\\ 0 & \text{otherwise}\end{cases}$. From (8), the above is also the c.c.d.f. of $\mathrm{SIR}_{km}^{(UL)}$.

B. Proof for Theorem 3

The Laplace transform of the downlink interference $I_{km}^{(DL)}$ is derive below.

$$\begin{aligned}
\mathcal{L}_{I_{km}^{(DL)}}(s) = \mathbb{E}\left[\mathrm{e}^{-s\bar{\alpha}_m\beta_{kkm}^2 R_{kkm}^{-2\epsilon}}\right] \times\\
\mathbb{E}\left[\prod_{l=1,\ l\neq k}^{\infty}\mathrm{e}^{-s(\bar{\alpha}_m+1)b_{kl}\beta_{lkm}^2 R_{lkm}^{-2\epsilon}}\right],
\end{aligned}$$

is obtained by noting that the two terms in (11) are independent of each other. Further, (12) is obtained by evaluating the expectation w.r.t. R_{kkm} in the first term of the above product, and then using the Campbell's theorem to evaluate the second theorem. Now, notice that the downlink SIR can be expressed as

$$\mathrm{SIR}_{km}^{(\mathrm{DL})} = \frac{1}{\bar{\alpha}_m + \frac{\bar{\alpha}_m+1}{\mathrm{SIR}_{km}}}, \tag{19}$$

where SIR_{km} denotes the SIR for the orthogonal pilots case studied in Section IV-A. Hence, the c.c.d.f. of $\mathrm{SIR}_{km}^{(\mathrm{DL})}$ is

$$\begin{aligned}
&\mathbb{P}\left(\left\{\mathrm{SIR}_{km}^{(\mathrm{DL})} > \gamma\right\}\right)\\
&= \mathbb{P}\left(\left\{\mathrm{SIR}_{km} > \bar{\gamma}\right\} \cap \left\{\gamma < \frac{1}{\bar{\alpha}_m}\right\}\right)
\end{aligned} \tag{20}$$

where $\bar{\gamma} = \left(\frac{\gamma(1+\bar{\alpha}_m)}{1-\bar{\alpha}_m\gamma}\right)$, and using the c.c.d.f. of SIR_{km} is obtained from (9) with $\eta = 1$.